

# Histological study on the effect of stem cells and hepatocyte growth factor on induced liver fibrosis in male albino rats

Abeer F. Abdel-Mohsen<sup>a</sup>, Nagla M. Salama<sup>a</sup>, Mohamed S. Elgendy<sup>b</sup> and Asmaa M. Elsayed<sup>b</sup>

<sup>a</sup>Histology Department, Faculty of Medicine, Cairo University, Cairo and <sup>b</sup>Histology Department, Faculty of Medicine Fayoum, University Fayoum University, Fayoum, Egypt

Corresponding to Dr. Mohamed S. Elgendy, MD, Department of Histology, Faculty of Medicine, Fayoum University, Fayoum 63514, Egypt  
Tel: +20 100 539 6843; fax: +20 846 302 350;  
e-mail: msg01@fayoum.edu.eg, drmohgendy@hotmail.com

Received 25 May 2014

Accepted 10 September 2014

The Egyptian Journal of Histology

2014, 37:615-628  
56 (1486-2014)

## Background

Liver fibrosis is a major Egyptian health problem. Hepatic stellate cells are the pivotal cells in the pathogenesis of liver fibrosis. Mesenchymal stem cells (MSCs) and hepatocyte growth factor (HGF) participate in liver fibrosis treatment; chitosan nanoparticles (CNPs) provide effective delivery of HGF to its niche.

## Aim of work

The aim of the study was to compare the effect of MSCs and HGF, either separately or mixed together, in improving liver fibrosis using a rat model of thioacetamide (TAA)-induced liver injury.

## Materials and methods

Sixty male albino rats were used in this work. They were divided into the control group and the TAA-induced fibrosis group, which was further subdivided into the untreated fibrosis group, the MSC-treated group, the HGF-incorporated CNP (HGF-CNP)-treated group, the MSCs+HGF-CNP-treated group, and the CNP-treated group. The livers were removed from sacrificed rats and processed for staining with H&E and Masson's trichrome and for immunohistochemical staining for  $\alpha$ -smooth muscle actin ( $\alpha$ -SMA) and proliferating cell nuclear antigen (PCNA).

## Results

The present study revealed that MSCs when mixed with HGF-CNP have a potent effect in improving TAA-induced liver fibrosis as regards restoration of the normal hepatic architecture and decreased collagen fiber content; positive  $\alpha$ -SMA immunoreaction was decreased with few immunoreactive hepatic stellate cells between hepatocytes. Many hepatocytes exhibited positive nuclear immunoreactivity for proliferating cell nuclear antigen. There was moderate improvement in the effect of MSCs or HGF-CNP alone. In contrast, CNPs achieved slight improvement in TAA-induced liver fibrosis.

## Conclusion

Coinjection of MSCs and HGF-CNP has a better therapeutic effect on liver fibrosis in rats compared with either one alone. This mode of therapy, if proved to be effective in humans, may provide a perfect alternative to liver transplantation.

## Keywords:

chitosan nanoparticle, hepatocyte growth factor, hepatic stellate cells, liver fibrosis, mesenchymal stem cells, thioacetamide

Egypt J Histol 37:615-628  
© 2014 The Egyptian Journal of Histology  
1110-0559

## Introduction

The liver is an important organ, responsible for metabolism, plasma protein synthesis, and detoxification. Liver fibrosis and cirrhosis result from chronic injury to the liver in conjunction with excessive deposition of collagen and other components of the extracellular matrix (ECM). Hepatic stellate cells (HSCs) play a principal role in liver fibrosis [1,2]. Many authors reported the regeneration of hepatocytes from stem cells. In-vivo transplantation of bone marrow mesenchymal stem cells (MSCs) in mice has been reported to improve cirrhosis [3,4]. The reason for

the transplantation of stem cells is to promote the regeneration of tissue-specific cells and subsequent morphological and functional recovery of organs of all lineage cells [5,6]. Hence, theoretically, bone marrow stem cells could be used in all disorders of mesodermal, ectodermal, and endodermal lineage tissues. This appears to provide exciting new opportunities for stem cell therapy. However, the number of stem cells engrafted and differentiated after transplantation limits the treatment roles. Furthermore, ambiguity continues over which subpopulation of bone marrow stem cells actually differentiates into hepatocytes and restores

the liver functions [7]. Moreover, the mechanism by which stem cells regenerate the respective parenchymal cells is not completely understood [8]. Evidence was reported for the transdifferentiation of stem cells [9]. Investigators attempted to improve cell therapy by means of several strategies such as delivery of bioactive molecules – for example, growth factors, cytokines, and chemokines [10]. Hepatocyte growth factor (HGF) has been reported to be a potent agent for acceleration of tissue regeneration following an acute insult, as well as for amelioration of tissue fibrosis and dysfunction in chronic conditions [11,12]. Although secretion of HGF after liver injury increases, long-term secretion in adults is questionable. The long-term effects of exogenous HGF remain questionable because of its short half-life period. As it is also cleared rapidly by the liver *in vivo*, exogenous HGF is extremely unstable in the blood circulation with a half-life of only 3–5 min [13,14]. This makes it almost impossible to sustain a constant high level of exogenous HGF in the circulation, even with repeated injections of HGF at short intervals. Nanotechnology offers solutions for the safe and conducive transportation of therapeutic proteins to the target site. Chitosan nanoparticles (CNPs), one among the biodegradable and less antigenic natural polymers, were reported to have the potential to carry and deliver biologically active macromolecules [15,16].

#### Aim of work

This work was designed to investigate the possible synergistic effect of HGF-incorporated CNP if coinjected with MSCs in improving experimental liver fibrosis and compare this with the possible effects of either MSCs or HGF-incorporated CNP separately.

#### Materials and methods

The original research was approved by the ethics committee in the Histology Department, Faculty of Medicine, Cairo University, Egypt, following international ethics and regulations for animal research in laboratory applications [17].

#### Materials

- (1) Thioacetamide (TAA) (catalog number: 6259; Loba Chemie, Mumbai, Maharashtra, India). It is in the form of crystalline powder in a 100 g bottle.
- (2) MSCs prepared from rat bone marrow (obtained from the stem cell research unit at the Biochemistry Department of the Faculty of Medicine, Cairo University (Cairo, Egypt) [18].
- (3) HGF (Koma Biotech, Seoul, Korea), catalog number: K0921103. The vial contains 10 µg of HGF in the form of recombinant, lyophilized protein.
- (4) Chitosan (CNP) (Sigma brand, catalog number: C3646; Sigma Aldrich, St Louis, Missouri, USA). It is in the form of powder in a 10 g bottle. The biological source of chitosan is shrimp shells and its degree of deacetylation (DD) is at least 75%.
- (5) HGF-incorporated CNP [19].

#### Chitosan nanoparticle preparation

- (1) 0.2% chitosan solution was prepared by dissolving 200 mg chitosan powder in 100 ml of 1% glacial acetic acid (Sigma Aldrich).
- (2) Nanoparticles were prepared by dropwise addition of 0.1% tripolyphosphate (Sigma Aldrich) solution in chitosan solution.
- (3) Turbidity was taken as an indicator for the formation of nanoparticles and the solution was subjected to centrifugation at 20 000 rpm for 20 min.
- (4) The supernatant was discarded.

#### Preparation of hepatocyte growth factor solution (according to Koma Biotech instructions)

- (1) The vial of recombinant HGF (Koma Biotech, Seoul, Korea) was centrifuged at 6000 rpm for 10 min at 4°C to bring the contents to the bottom.
- (2) The content of the vial was reconstituted with sterile distilled water to make a concentration of 10 µg/ml to be stored at –20°C for further use. A volume of 0.1 ml of this solution contained 1000 ng of HGF, which was added to 10 ml of chitosan stock solution to make HGF–CNP solution; each 1 ml contained 100 ng of HGF [23].

MSCs were labeled with PKH26 (named after its discovery by Paul Karl Horan) red fluorescent cell linker mini kit for general cell membrane labeling (Sigma brand, catalog number: MINI26; Sigma Aldrich). It is in the form of PKH26 dye stock solution (one vial containing 0.1 ml,  $1 \times 10^{-3}$  mol/l in ethanol) and diluent C (one vial containing 10 ml). This was done to ensure homing of MSCs and trace the injected cells into the liver tissue (according to Sigma protocol).

#### Animals

Sixty adult male albino rats weighing 175–225 g were used in this study. The animals were locally bred at the animal house of the Faculty of Medicine, Cairo University, in hygienic stainless steel cages in a clean well-ventilated room. Standard laboratory chow and tap water were available.

Animals were divided into two main groups:

- (1) *Group I (the control group)*: this group consisted of 10 rats. They were injected intraperitoneally with 1 ml of sterile distilled water three times a week for 8 weeks. After this time period, they were injected with 1 ml PBS in a single dose in the tail vein.
- (2) *Group II (the fibrosis group)*: this group consisted of 50 rats. They received intraperitoneal injection of 200 mg/kg of TAA dissolved in 1 ml sterile distilled water three times a week for 8 weeks to induce liver fibrosis. After this time period, the rats were further subdivided into five subgroups of 10 rats each:
  - (a) *Subgroup IIa* (the untreated fibrosis group): the rats in this group were injected only with a single dose of 1 ml PBS in the tail vein.
  - (b) *Subgroup IIb* (the MSCs-treated group): the rats in this group received a single injection of  $1 \times 10^6$  of MSCs labeled with PKH26 dye in 1 ml PBS in the tail vein.

- (c) *Subgroup IIc* (the HGF–CNP-treated group): The rats in this group received a single injection of HGF–CNP at a dose of 100 ng of HGF in 1 ml CNP solution in the tail vein.
- (d) *Subgroup IIId* (the MSCs+HGF–CNP-treated group): the rats in this group received a single injection of  $1 \times 10^6$  PKH26-labeled MSCs in 1 ml PBS mixed with HGF–CNP at a dose of 100 ng of HGF in 1 ml CNP solution in the tail vein.
- (e) *Subgroup IIe* (the CNP-treated group): the rats in this group received a single injection of 1 ml CNP solution in the tail vein.

### Methods

Four weeks after all injections, rats from all groups were anesthetized using intraperitoneal injection of phenobarbitone at 60 mg/kg and then sacrificed. Liver specimens were taken rapidly and processed to prepare paraffin sections. Serial sections of 7  $\mu$ m thickness were cut and subjected to the following stains:

- (1) PKH26 labeling of MSCs: a fluorescent microscope was used to confirm homing of PKH26-labeled MSCs.
- (2) H&E stain to examine the general histological changes of the liver [20].
- (3) Masson's trichrome stain to detect changes in collagen fiber content in different groups [20].
- (4) Immunohistochemical staining of  $\alpha$ -smooth muscle actin ( $\alpha$ -SMA) and proliferating cell nuclear antigen (PCNA).

Mouse monoclonal antibody was used against:

- (1)  $\alpha$ -SMA (catalog number: MS-113-R7) as a marker of activated HSCs.
- (2) PCNA (catalog number: MS-106-R7) as a marker of hepatocyte regeneration.

The kits were obtained from NeoMarkers (Lab Vision Corporation, Westinghouse, California, USA).

### Immunohistochemical staining

These anti-rat monoclonal antibodies are suitable for immunohistochemical staining of formalin-fixed paraffin-embedded sections using the avidin–biotin peroxidase complex technique.

Sections were dewaxed in xylene, rehydrated, and pretreated with 3% hydrogen peroxide for blocking endogenous peroxidase activity. Microwave-assisted antigen retrieval was then performed for 20 min. Sections were incubated overnight at 40°C with the corresponding antibody. After washing with PBS, sections were incubated with biotinylated IgG and then with streptavidin–peroxidase conjugate. Sections were then washed with PBS and incubated with diaminobenzidine for 5 min and counterstained with Mayer's hematoxylin. Positive cells for  $\alpha$ -SMA showed cytoplasmic brown deposits. Positive cells for PCNA showed nuclear brown staining. To obtain negative controls, additional specimens of the liver were processed in the same way but omitting the primary antibody. Positive control was

a specimen of pylorus for  $\alpha$ -SMA and a specimen of the tonsil for PCNA [21].

### Quantitative morphometric analysis

The following parameters were examined using Leica Qwin 500 Image analysis (Hessen, Wetzlar, Germany): For each parameter, measurements were taken in five randomly selected nonoverlapping fields per slide from five slides of each animal.

- (1) *Area percentage of collagen*: it was measured from sections from all groups using an objective lens of magnification 4 (a total magnification of 40).
- (2) *Area percentage of  $\alpha$ -SMA*: it was measured from sections from all groups using an objective lens of magnification 10 (a total magnification of 100). Fields containing apparent blood vessels were avoided.
- (3) *Number of PCNA-immunopositive hepatocytes*: interactive counting of immunopositive cells was done using an objective lens of magnification 40 (total magnification of 400).

### Statistical analysis

Statistical analysis was performed using SPSS software (Chicago, USA). Data were presented as mean $\pm$ SD. Differences among the study groups were detected by one-way analysis of variance as a global test to determine any differences in data before comparing pairs of groups; thereafter, the *t*-test was used to compare two groups. *P* values less than 0.05 were considered statistically significant [22].

## Results

### Histological results

#### Group I (control group)

Examination of the liver tissue of group I (control group) with H&E revealed ill-defined hepatic lobules formed of cords of hepatocytes radiating from the central vein to the periphery of the lobule. The portal areas contained branches of bile duct lined with simple cubical epithelium, a branch of portal vein, which is the widest with a thin wall, and a branch of hepatic artery that is rounded with narrow lumen. The hepatocytes appeared as polygonal cells having acidophilic cytoplasm and central rounded vesicular nuclei with prominent nucleoli. Some cells were binucleated. Hepatocyte cords were separated by blood sinusoids (Fig. 1). Staining with Masson's trichrome showed minimal amount of collagen fibers around the central vein and in the portal tracts with unremarkable interlobular septa demarcating the classic hepatic lobules (Fig. 2). Immunoreaction to  $\alpha$ -SMA was seen in the media of central veins and in the vessels of the portal area. No positive immunostained cells were detected between the hepatocytes. As regards PCNA immunostaining most fields showed no immunopositive hepatocytes. However, in some fields, only one or two hepatocytes showed brown nuclear immunoreaction (Fig. 3).

*Group II (the fibrosis group)*

H&E-stained liver tissue of the rats in subgroup IIa that received TAA showed marked thickening of the interlobular septa with inflammatory cellular infiltration and marked dilatation of the portal veins and disorganization of the lobular architecture. Hepatocytes showed acidophilic cytoplasm. Some cells were binucleated and some vacuolated hepatocytes could also be detected (Fig. 4). Staining with Masson's trichrome revealed marked increase in the amount of collagen fibers in the interlobular septa, portal tracts, and in between the distorted hepatocyte cords (Fig. 5). There were large numbers of HSCs showing positive immunostaining for  $\alpha$ -SMA. HSCs appeared as branched, stellate cells, situated between the hepatocytes. A few hepatocytes showed positive nuclear immunoreaction for PCNA (Fig. 6).

Liver tissue of the rats in subgroup IIb (MSCs-treated group) stained with H&E showed thickening of the connective tissue septa and dilated portal vessels with inflammatory cellular infiltration, but these changes were moderate in comparison with those of subgroup IIa. Most hepatocytes had normal appearance with vesicular nuclei, and some binucleated hepatocytes were also detected (Fig. 7). Staining with Masson's trichrome showed relatively small amounts of collagen in the connective tissue septa between hepatic lobules and in the portal areas (Fig. 8). There was positive  $\alpha$ -SMA immunoreactivity in the media of the blood vessels. Some  $\alpha$ -SMA-positive HSCs were detected between the hepatocytes and in the portal area. HSCs appeared stellate shaped with fine processes that extended between the hepatocytes. Many hepatocytes exhibited positive nuclear immunoreactivity for PCNA (Fig. 9).

Liver tissue of the rats in subgroup IIc (the HGF-CNP-treated group) stained with H&E showed thickening of the interlobular fibrous septa with dilated portal vessels and disorganization of the lobular architecture but to less extent compared with subgroup IIa. There were many normal hepatocytes with vesicular nuclei. A few vacuolated hepatocytes could be seen. Some hepatocytes with rarified cytoplasm and lost outlines were detected. A few cells with deep acidophilic cytoplasm and dark small pyknotic nuclei were also noticed. Mild cellular infiltration was also detected between the hepatocytes (Fig. 10). Staining with Masson's trichrome showed a moderate to large amount of collagen within the connective tissue septa and in the portal areas (Fig. 11). There was positive  $\alpha$ -SMA immunoreactivity in the media of the portal blood vessels and in HSCs in between the hepatocytes. Many hepatocytes showed positive nuclear immunoreactivity for PCNA (Fig. 12).

Liver tissue of the rats in subgroup IId (MSCs+HGF-CNP-treated group) stained with H&E showed marked improvement in the hepatic architecture. Cords of hepatocytes with vesicular nuclei were seen radiating from the central vein. There was absence of dilated vessels in the portal tract; however, remnants of thin connective tissue septa were found. A few hepatocytes

with deep acidophilic cytoplasm and dark small pyknotic nuclei were detected. Many binucleated hepatocytes could be seen (Fig. 13). Staining with Masson's trichrome showed minimal amounts of collagen fibers around the central vein and in the portal tracts, which were comparable to the control group (Fig. 14). The positive  $\alpha$ -SMA immunoreaction was detected mainly in the media of blood vessels. Only a few HSCs exhibited faint immunoreaction between hepatocytes. Many hepatocytes exhibited positive nuclear immunoreactivity for PCNA (Fig. 15).

Liver tissue of the rats in subgroup IIe (the CNP-treated group) stained with H&E showed marked thickening of the interlobular septa and disorganization of the lobular architecture. Many hepatocytes were vacuolated with fragmented nuclei (karyorrhexis). Some cells with deep acidophilic cytoplasm and dark small pyknotic nuclei were also noticed (Fig. 16). Staining with Masson's trichrome showed a large amount of collagen fibers in the interlobular septa and between hepatocytes (Fig. 17). There were abundant HSCs that were positively immunostained for  $\alpha$ -SMA in between the hepatocytes. A few hepatocytes showed positive immunoreaction for PCNA (Fig. 18).

**Morphometric results**

Analysis of variance among groups with respect to the mean area% of collagen, the mean area% of  $\alpha$ -SMA immunoreactivity, and the mean number of PCNA-reactive cells showed a statistically significant variance among the groups in each parameter ( $P < 0.05$ ).

A comparison between two groups with respect to these parameters was performed using the *t*-test and the results have been summarized in Tables 1–3 and Histograms 1–3.

Table 1 and Histogram 1 summarize the results of the mean area% of collagen.

The greatest area% of collagen was detected in group IIa (the untreated fibrosis group), whereas the smallest was in group I (control group). Comparison between two groups revealed a statistically significant difference ( $P < 0.05$ ) except between the following pairs:

- (1) Group I (the control group) and subgroup IId (the MSCs+HGF-CNP-treated group).
- (2) Subgroup IIb (the MSCs-treated group) and subgroup IIc (the HGF-CNP-treated group).

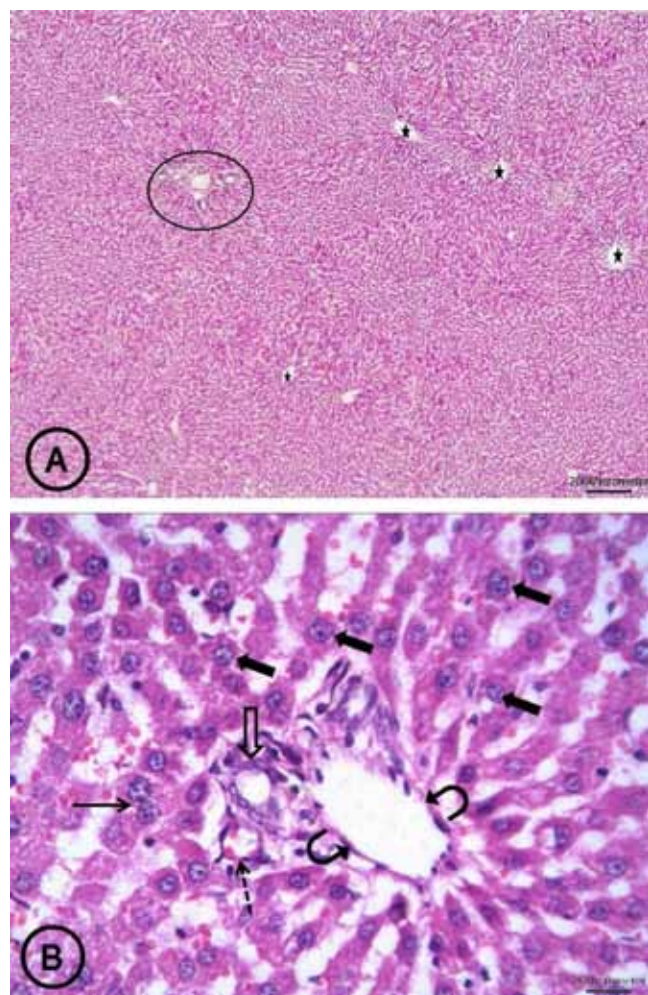
Table 2 and Histogram 2 summarize the results of the mean area% of  $\alpha$ -SMA immunoreactivity.

The mean area% of  $\alpha$ -SMA immunoreactivity revealed the highest value in group IIa (the untreated fibrosis group) and the least in group I (the control group). Comparison between two groups revealed a statistically significant difference ( $P < 0.05$ ) except between the following groups:

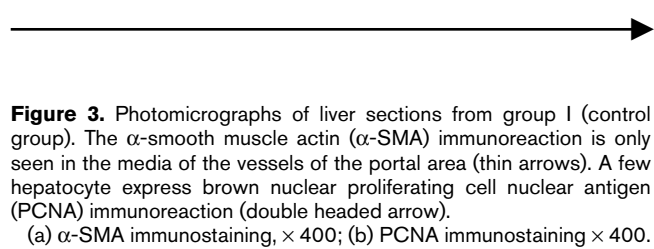
- (1) Group I (the control group), subgroup IIb (the MSCs-treated group), and subgroup IId (the MSCs+HGF-CNP-treated group).

Table 3 and Histogram 3 summarize the results of the mean number of PCNA-positive hepatocytes.

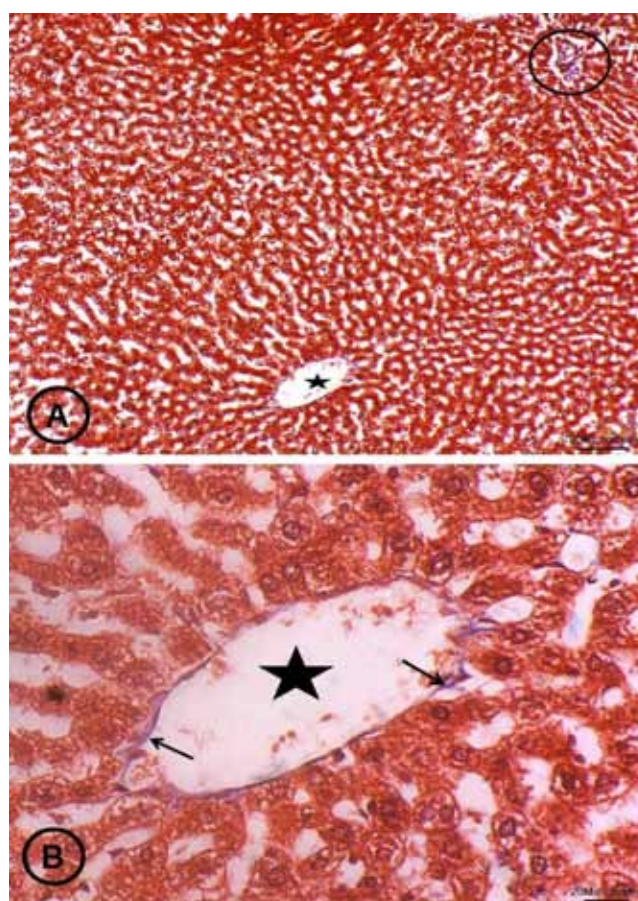
The mean number of PCNA-positive hepatocytes revealed the highest value in subgroup II d (the MSCs+HGF-CNP-treated group), whereas the least was in group I (the control group). A comparison between two groups revealed a statistically significant difference ( $P < 0.05$ ).



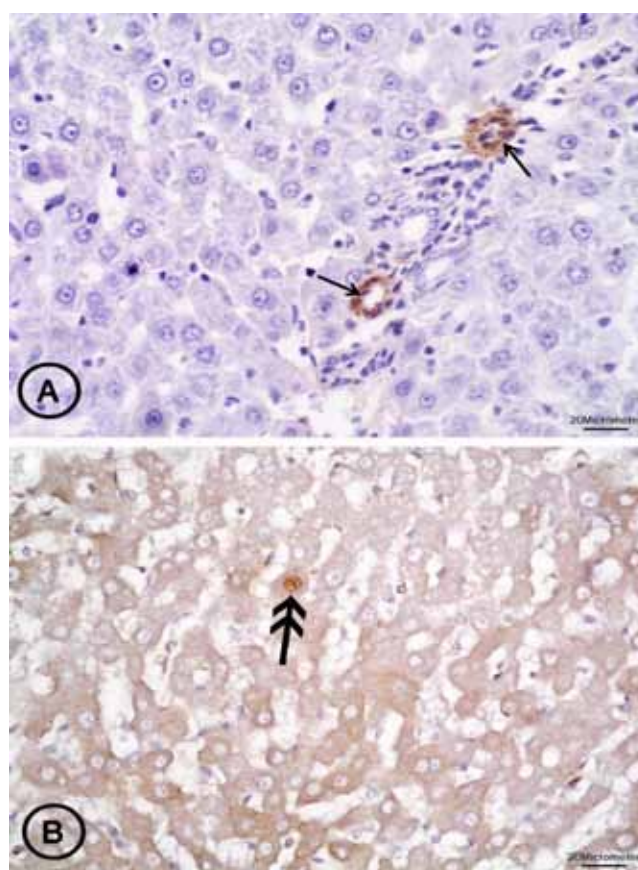
**Figure 1.** Photomicrographs of liver sections from group I (the control group) showing ill-defined lobulation with central veins (stars), radiating cords of hepatocytes, and portal area (encircled). The portal area has a branch of bile duct lined with simple cubical epithelium (hollow arrow), a branch of the portal vein having a thin wall and wide lumen (curved arrows), and branch of the hepatic artery (dotted arrow). The hepatocytes have vesicular nuclei with prominent nucleoli (thick arrows); some are binucleated (thin arrow).  
H&E, (a)  $\times 40$ ; (b)  $\times 400$ .



**Figure 3.** Photomicrographs of liver sections from group I (control group). The  $\alpha$ -smooth muscle actin ( $\alpha$ -SMA) immunoreaction is only seen in the media of the vessels of the portal area (thin arrows). A few hepatocyte express brown nuclear proliferating cell nuclear antigen (PCNA) immunoreaction (double headed arrow).  
(a)  $\alpha$ -SMA immunostaining,  $\times 400$ ; (b) PCNA immunostaining  $\times 400$ .



**Figure 2.** Photomicrographs of liver sections from group I (control group) showing minimal collagen (thin arrows) around the central vein (star) and in the portal tract (encircled).  
Masson's trichrome, (a)  $\times 100$ ; (b)  $\times 400$ .



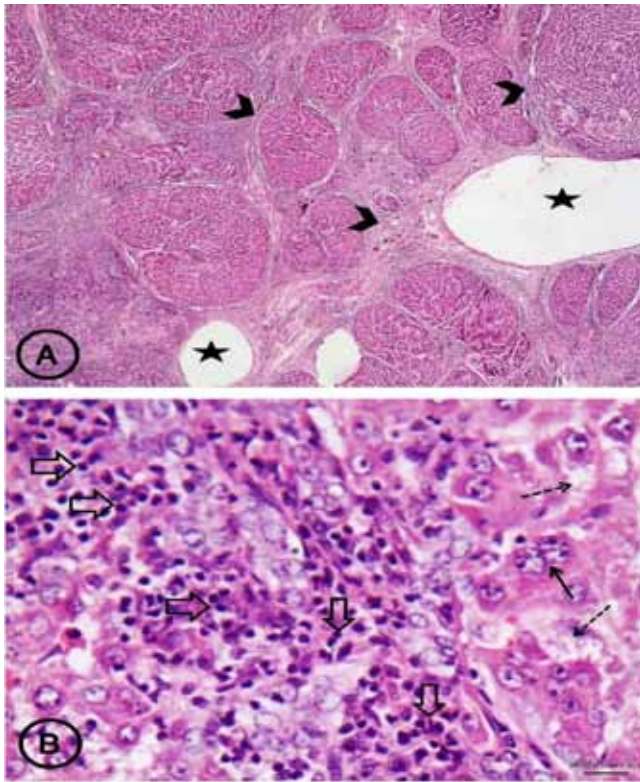


**Figure 4.** Photomicrographs of liver sections from subgroup IIa (the untreated fibrosis group) showing marked thickening of the fibrous septa in between the hepatic lobules (arrow heads) with disorganization of the lobular architecture. Notice the marked dilatation of the portal veins (stars). There is heavy inflammatory cellular infiltration (hollow arrows). Some hepatocytes appear vacuolated (dotted arrows) or binucleated (thin arrow).  
H&E, (a)  $\times 40$ ; (b)  $\times 400$ .

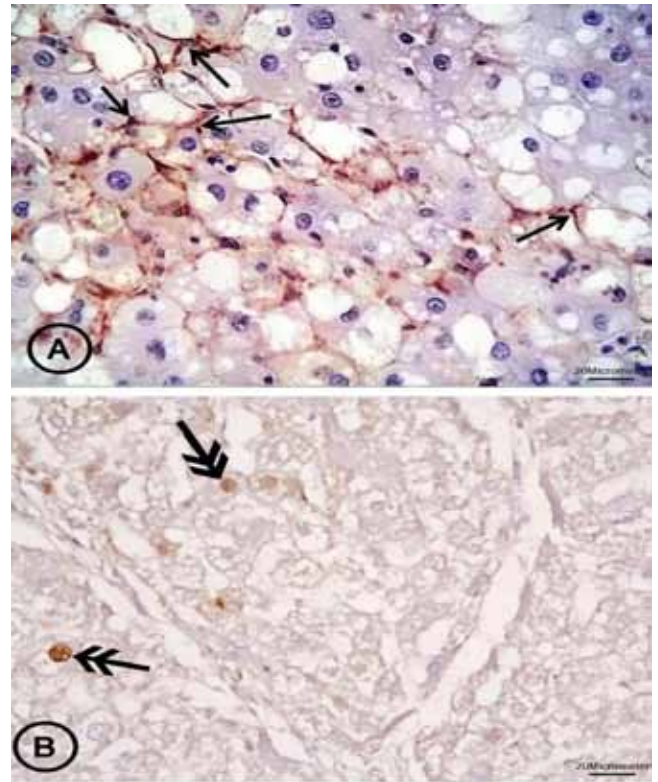


**Figure 6.** Photomicrographs of liver sections from subgroup IIa (the untreated fibrosis group) showing  $\alpha$ -SMA immunoreactive cells that are stellate shaped with fine processes that extend between the hepatocytes (thin arrows). A few hepatocytes express positive nuclear proliferating cell nuclear antigen (PCNA) immunoreaction (double headed arrows). (a)  $\alpha$ -SMA immunostaining,  $\times 400$ ; (b) PCNA immunostaining,  $\times 400$ .

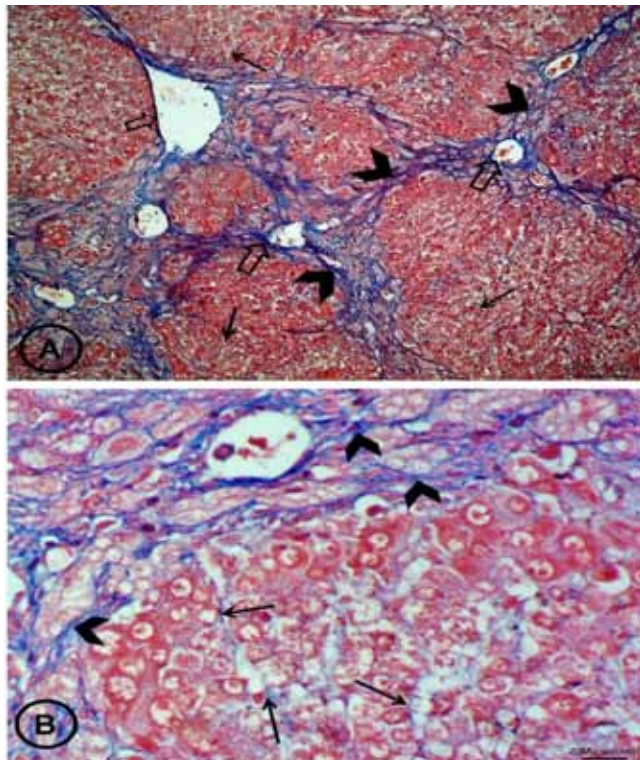


**Figure 5.** Photomicrographs of liver sections from subgroup IIa (the untreated fibrosis group) showing extensive collagen fibers in the connective tissue septa between the hepatic lobules (arrow heads), in the portal areas (hollow arrows), and in between the hepatocytes (thin arrows).  
Masson's trichrome, (a)  $\times 100$ ; (b)  $\times 400$ .

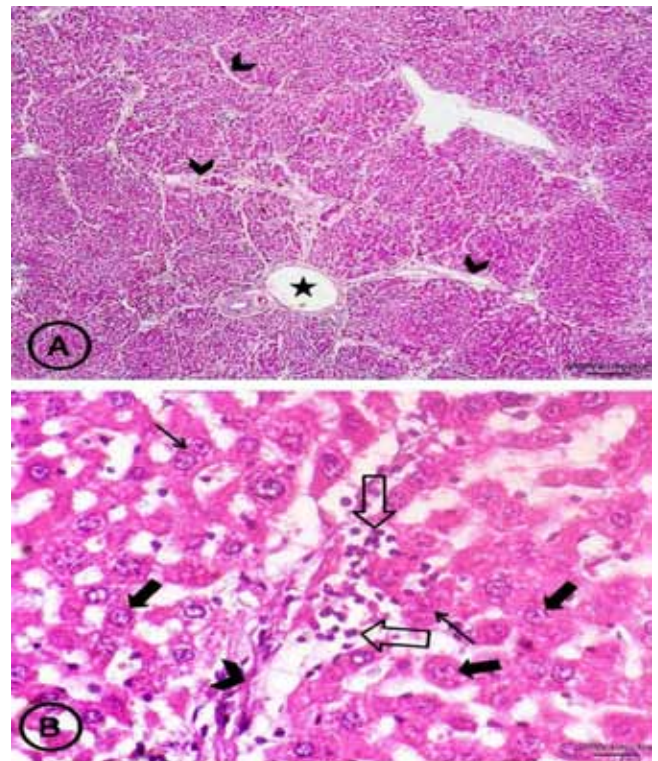


**Figure 7.** Photomicrographs of liver sections from subgroup IIb (the MSCs-treated group) showing moderately thickened connective tissue septa (arrow heads) and dilated portal vessel (star). There is mild cellular infiltration (hollow arrows). Most hepatocytes have vesicular nuclei (thick arrows) and some are binucleated (thin arrows).  
H&E (a)  $\times 40$ ; (b)  $\times 400$ .

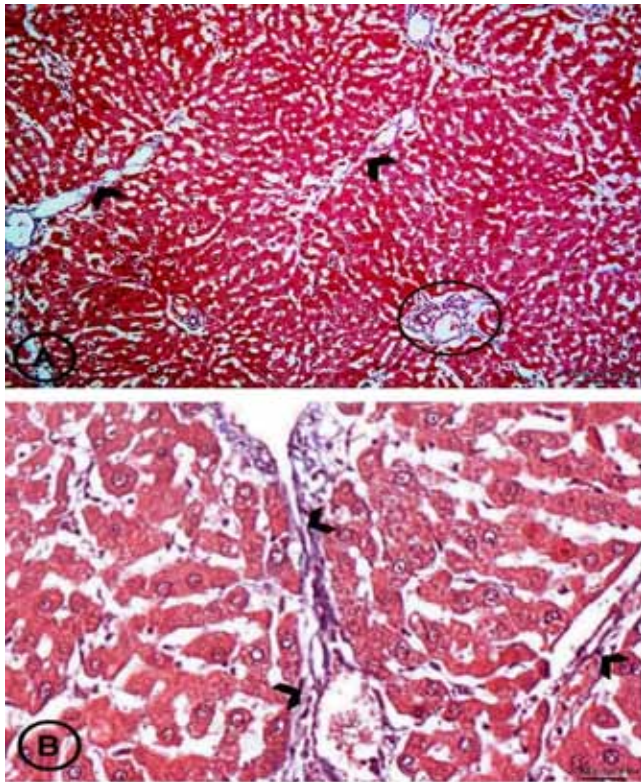


**Figure 8.** Photomicrographs of liver sections from subgroup IIb (the MSCs-treated group) showing relatively small amount of collagen fibers in the septa between hepatic lobules (arrow heads) and in the portal area (encircled).

Masson's trichrome (a)  $\times 100$ ; (b)  $\times 400$ .

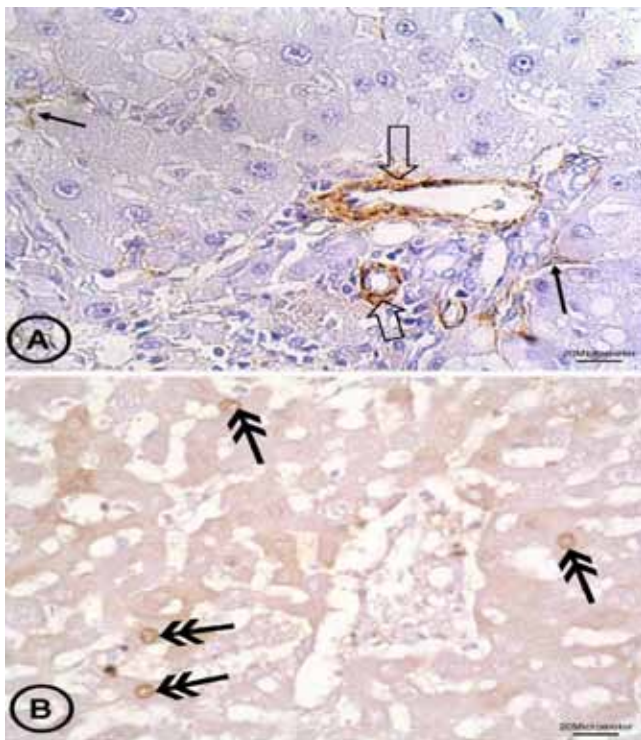


**Figure 9.** Photomicrographs of liver sections from subgroup IIb (the MSCs-treated group) showing  $\alpha$ -smooth muscle actin ( $\alpha$ -SMA) immunoreactive cells that are stellate in shape with fine processes that extend between the hepatocytes (thin arrows). The media of the blood vessels in the portal tract are also  $\alpha$ -SMA immunoreactive (hollow arrows). Some hepatocytes express positive nuclear proliferating cell nuclear antigen (PCNA) immunoreactions (double headed arrows).

(a)  $\alpha$ -SMA immunostaining,  $\times 400$ ; (b) PCNA immunostaining,  $\times 400$ .

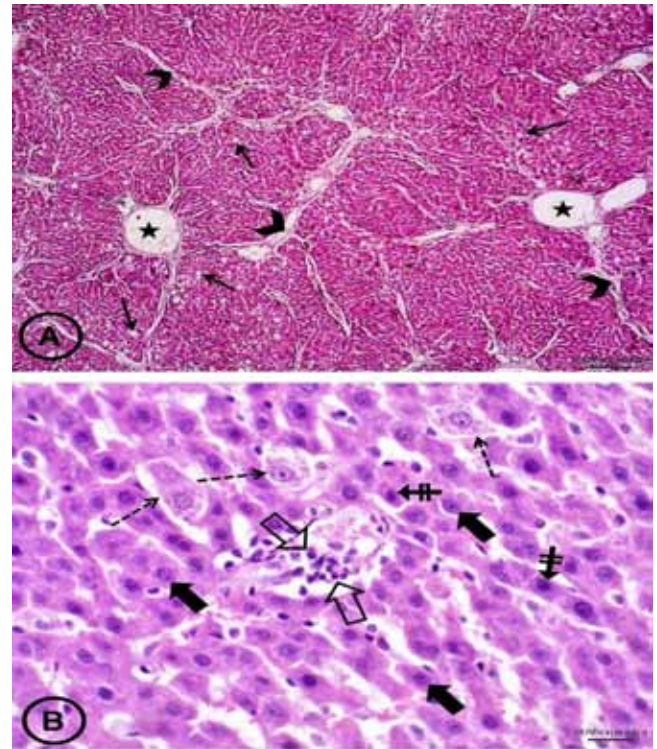


**Figure 10.** Photomicrographs of liver sections from subgroup IIc (the HGF-CNP-treated group) showing thickening of the connective tissue septa (arrow heads) with disorganization of the hepatic architecture. Note the presence of a few vacuolated hepatocytes (thin arrows) and dilated portal vessels (stars). There are many normal hepatocytes with vesicular nuclei (thick arrows). Some hepatocytes show rarified cytoplasm (dotted arrows). A few cells with deep acidophilic cytoplasm and small dark pyknotic nuclei are also seen (crossed arrows). There is mild cellular infiltration (hollow arrows).

H&E (a)  $\times 40$ ; (b)  $\times 400$ .

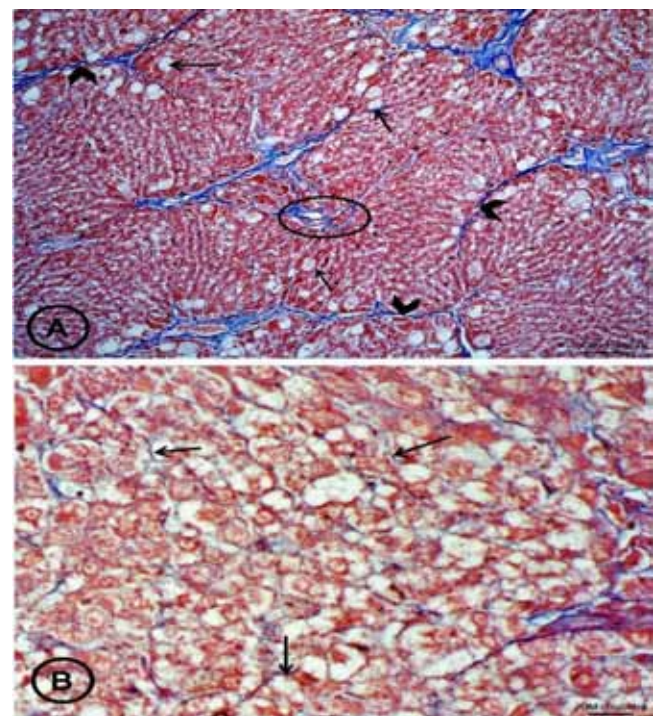


**Figure 11.** Photomicrographs of liver sections from subgroup IIc (the HGF-CNP-treated group) showing a moderate amount of collagen in the connective tissue septa (arrow heads) and in the portal area (encircled). There is a moderate amount of collagen between many vacuolated hepatocytes (thin arrows).

Masson's trichrome (a)  $\times 100$ ; (b)  $\times 400$ .

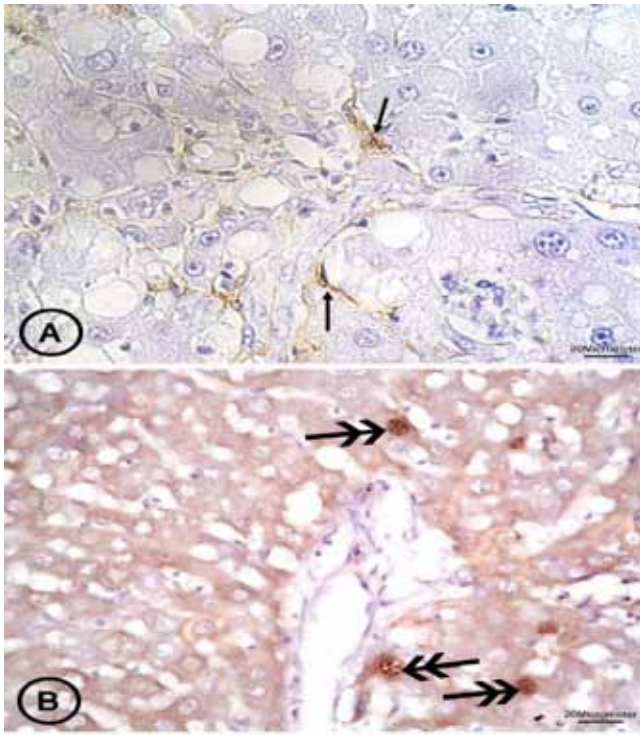


**Figure 12.** Photomicrographs of liver sections from subgroup IIc (the HGF-CNP-treated group) showing  $\alpha$ -SMA immunoreactive cells that are stellate shaped with fine processes that extend between the hepatocytes (thin arrows). A few hepatocytes express positive nuclear proliferating cell nuclear antigen (PCNA) immunoreaction (double headed arrows).  
(a)  $\alpha$ -SMA immunostaining,  $\times 400$ ; (b) PCNA immunostaining,  $\times 400$ .

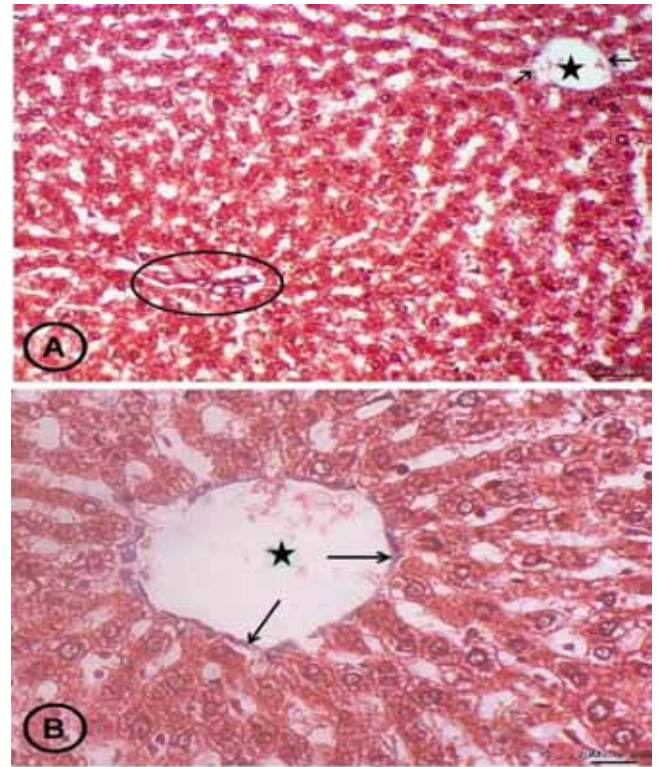


**Figure 14.** Photomicrographs of liver sections from subgroup IIId (the MSCs+HGF-CNP-treated group) showing minimal collagen (thin arrows) around the central vein (stars) and in the portal tract (encircled).  
Masson's trichrome (a)  $\times 100$ ; (b)  $\times 400$ .

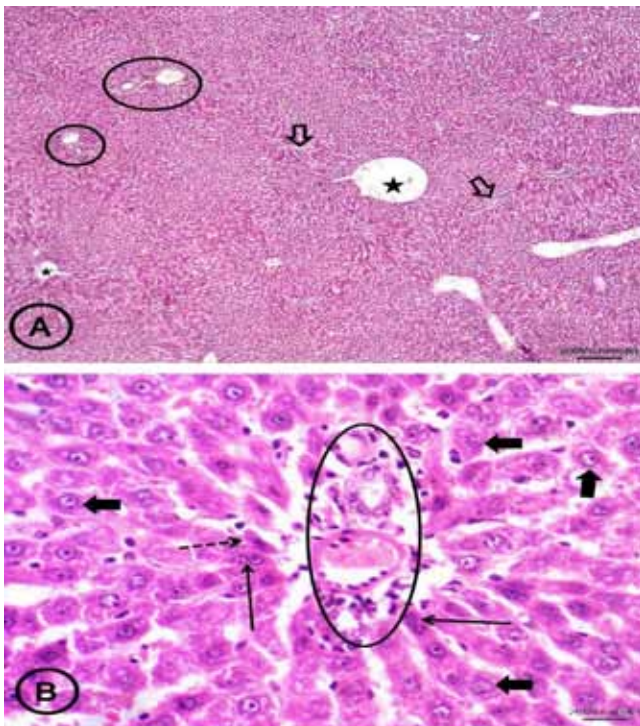


**Figure 13.** Photomicrographs of liver sections from subgroup IIId (the MSCs+HGF-CNP-treated group) showing normal hepatic architecture with cords of hepatocytes radiating from the central vein (star). Connective tissue septa are thin (hollow arrows); portal areas (encircled) appear normal. Most hepatocytes appear normal with vesicular nuclei (thick arrows), whereas some cells have deep acidophilic cytoplasm with dark nuclei (dotted arrow) and some others are binucleated hepatocytes (thin arrows).  
H&E (a)  $\times 40$ ; (b)  $\times 400$ .

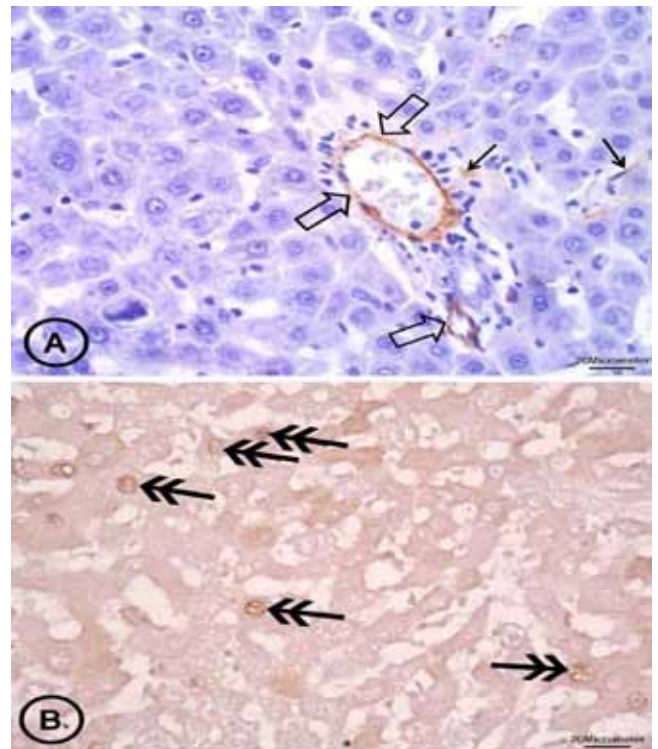


**Figure 15.** Photomicrographs of liver sections from subgroup IIId (the MSCs+HGF-CNP-treated group) showing that  $\alpha$ -SMA immunoreaction is mainly seen in the media of blood vessels in the portal tract (hollow arrows). A few faintly immunostained HSCs (thin arrows) are seen extending between hepatocytes. Many hepatocytes express positive nuclear proliferating cell nuclear antigen (PCNA) immunoreaction (double headed arrows).  
(a)  $\alpha$ -SMA immunostaining,  $\times 400$ ; (b) PCNA immunostaining,  $\times 400$ .

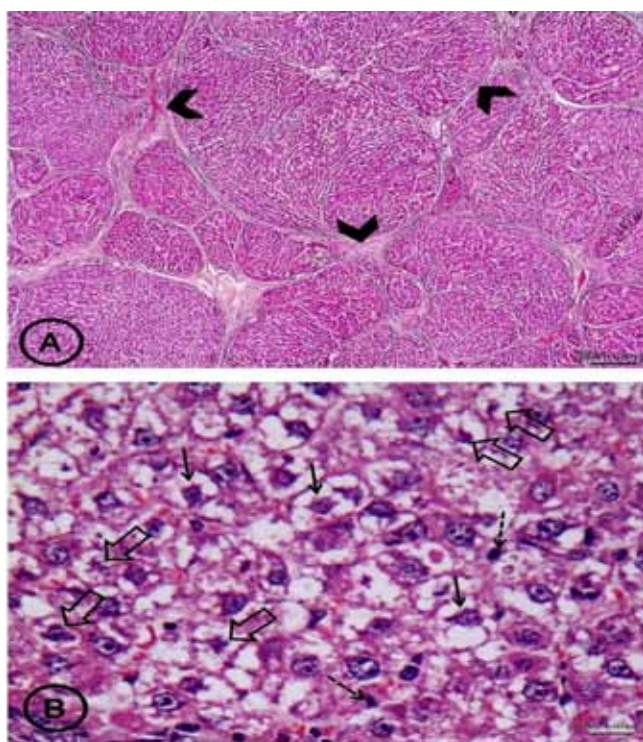


**Figure 16.** Photomicrographs of liver sections from subgroup IIe (the CNP-treated group) showing thickening of the fibrous septa between the hepatic lobules (arrow heads) with disorganization of the lobular architecture. There are many vacuolated hepatocytes (thin arrows). Some cells appear with deep acidophilic cytoplasm and small, dark pyknotic nuclei (dotted arrow), whereas some other cells show fragmented nuclei in vacuolated hepatocytes (hollow arrows).  
H&E (a)  $\times 40$ ; (b)  $\times 400$ .

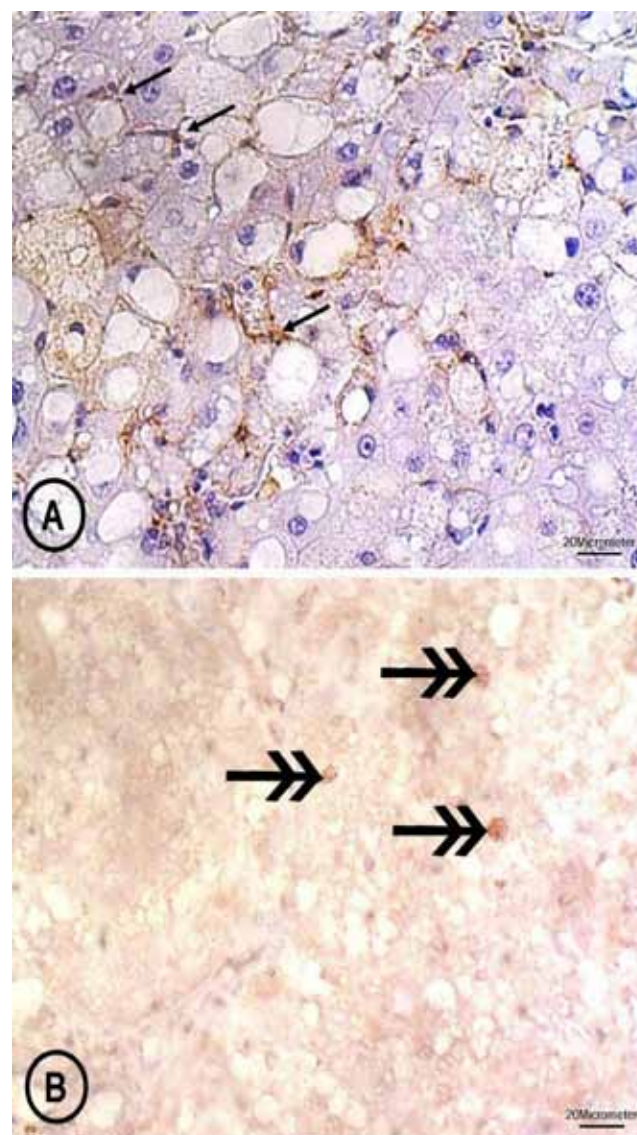
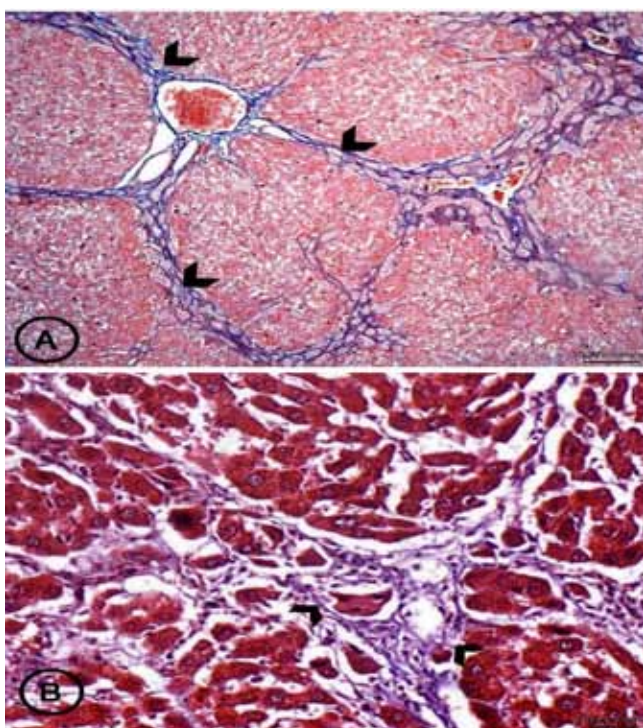


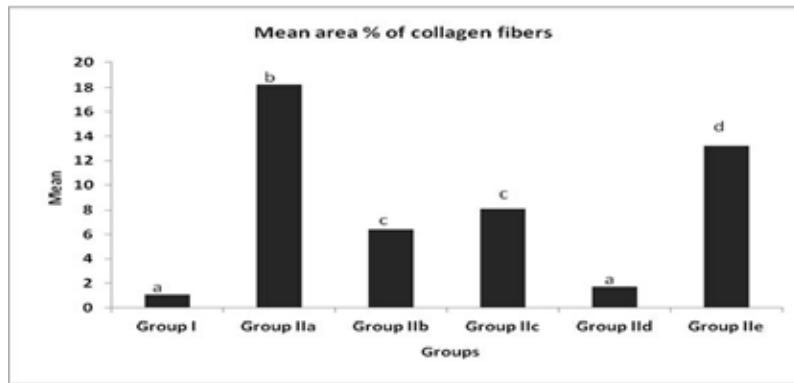
**Figure 18.** Photomicrographs of liver sections from subgroup IIe (the CNP-treated group) showing many  $\alpha$ -SMA immunoreactive HSCs that are stellate shaped with fine processes that extend between the hepatocytes (thin arrows). A few hepatocytes express positive nuclear proliferating cell nuclear antigen (PCNA) immunoreaction (double headed arrows).  
(a)  $\alpha$ -SMA immunostaining,  $\times 400$ ; (b) PCNA immunostaining,  $\times 400$ .

**Figure 17.** Photomicrographs of liver sections from subgroup IIe (the CNP-treated group) showing extensive collagen fiber deposition in the septa between the hepatic lobules (arrow heads).  
Masson's trichrome (a)  $\times 100$ ; (b)  $\times 400$ .

**Table 1. Area% (mean $\pm$ SD) of collagen fibers**

Groups	Group I (control)	Group IIa (untreated fibrosis)	Group IIb (MSCs treated)	Group IIc (HGF-CNP treated)	Group IIe (MSCs+HGF-CNP treated)	Group IIe (CNP treated)
Mean $\pm$ SD	1.09 $\pm$ 0.59 <sup>a</sup>	18.23 $\pm$ 5.22 <sup>b</sup>	6.45 $\pm$ 1.11 <sup>c</sup>	8.11 $\pm$ 1.35 <sup>c</sup>	1.73 $\pm$ 1.44 <sup>a</sup>	13.22 $\pm$ 3.54 <sup>d</sup>

Different superscripts indicate statistically significant difference ( $P < 0.05$ ) compared with other groups. CNP, chitosan nanoparticle; HGF, hepatocyte growth factor; MSC, mesenchymal stem cell.

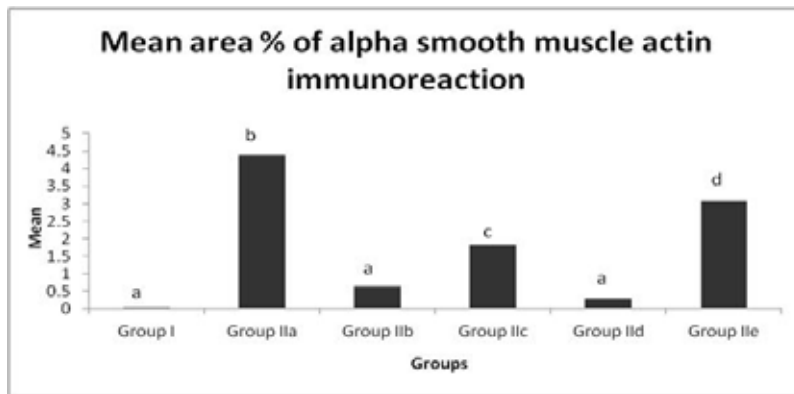


**Histogram 1.** Mean area% of collagen fibers. Different superscripts indicate statistically significant difference ( $P < 0.05$ ) compared with other groups.

**Table 2. Area% (mean±SD) of  $\alpha$ -smooth muscle actin immunoreaction**

Groups	Group I (control group)	Group IIa (untreated fibrosis group)	Group IIb (MSCs treated group)	Group IIc (HGF-CNP treated group)	Group IId (MSCs+HGF-CNP treated group)	Group IIe (CNP treated group)
Mean±SD	0.05 ± 0.09 <sup>a</sup>	4.38 ± 1.33 <sup>b</sup>	0.63 ± 0.25 <sup>a</sup>	1.83 ± 0.88 <sup>c</sup>	0.27 ± 0.17 <sup>a</sup>	3.07 ± 1.71 <sup>d</sup>

Different superscripts indicate statistically significant difference ( $P < 0.05$ ) compared with other groups. CNP, chitosan nanoparticle; HGF, hepatocyte growth factor; MSC, mesenchymal stem cell.

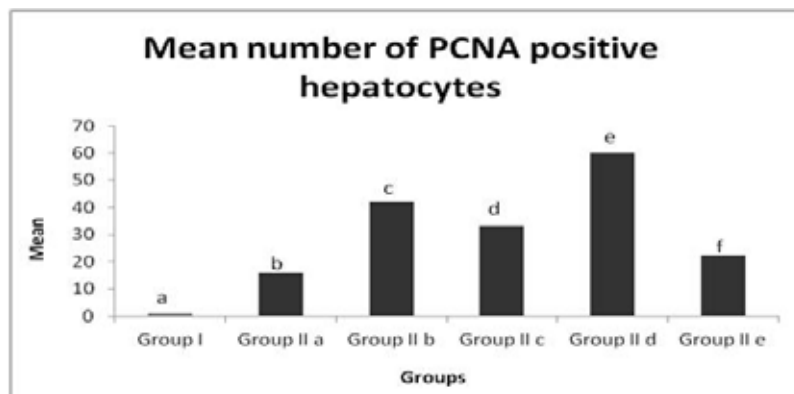


**Histogram 2.** Mean area% of  $\alpha$ -smooth muscle actin immunoreaction. Different superscripts indicate statistically significant difference ( $P < 0.05$ ) compared with other groups.

**Table 3. Number (mean±SD) of proliferating cell nuclear antigen positive hepatocytes**

Group	Group I	Group IIa	Group IIb	Group IIc	Group IId	Group IIe
Mean±SD	0.7 ± 0.82 <sup>a</sup>	16.2 ± 0.92 <sup>b</sup>	42.1 ± 2.02 <sup>c</sup>	33.3 ± 7.06 <sup>d</sup>	59.9 ± 2.08 <sup>e</sup>	22.3 ± 2.11 <sup>f</sup>

Different superscripts indicate statistically significant difference ( $P < 0.05$ ) compared with other groups.



**Histogram 3.** Mean number of proliferating cell nuclear antigen-positive hepatocytes. Different superscripts indicate statistically significant difference ( $P < 0.05$ ) compared with other groups.

## Discussion

Liver fibrosis is caused by chronic liver injury, resulting in excessive deposition of collagen and other components of ECM [1,2].

Stem cell transplantation is an attractive line in regenerative medicine. HGF is a crucial mitogen and morphogen for liver regeneration process after liver injuries [23].

The present study aimed to investigate the therapeutic effect of MSCs, HGF, and the combination of both on liver fibrosis.

Rodent models for liver fibrosis can be induced by a variety of hepatotoxins. However, TAA was used in this study as the resultant fibrosis is similar to that of chronic hepatitis infection, which is a highly prevalent disease, especially in Egypt, and is comparable to liver cirrhosis in humans [24]. The dosage and duration was determined according to the pilot study and in accordance with Alshawsh *et al.* [25].

In this study, MSCs, HGF–CNP, MSCs+HGF–CNP, and CNP were administered by the intravenous route as it is the least invasive route and the most effective [26].

Identification of activated HSCs was performed using immunohistochemical staining for  $\alpha$ -SMA, as it has been proved to be a reliable and widely used marker of HSC activation [27]. HSC activation is an early step in liver fibrogenesis; this is followed by collagen deposition and progressive fibrosis, leading to cirrhosis [28]. Immunohistochemical detection of PCNA was also performed in this work as a marker of hepatocyte proliferation [29].

Minimal amount of collagen fibers around the central vein and in portal tracts was detected by Masson's trichrome staining. No interlobular septa could be detected demarcating the hepatic lobules. These findings were in agreement with those of Alshawsh *et al.* [25].

In the control group, immunoreaction to  $\alpha$ -SMA was seen only in the media of the central vein and vessels of portal areas, which is attributed to the smooth muscles within the media. No positive immunostained cells in between hepatocytes were detected. This absence of  $\alpha$ -SMA-positive HSCs could explain the absence of collagen fibers in between the hepatocytes [30]. Few hepatocytes expressed positive immunoreaction for PCNA, which coincides with the results of Gu *et al.* [31], who detected a few PCNA-positive hepatocytes in normal livers of mice.

Subgroup IIa (the untreated fibrosis group) showed extensive loss of normal hepatic architecture in the form of marked thickening of the interlobular septa associated with heavy inflammatory cellular infiltration and marked dilatation of the portal vessels. Some hepatocytes had deep acidophilic cytoplasm and pyknotic nuclei, which were indicative for apoptosis; other hepatocytes appeared vacuolated and might contain fragmented nuclei, which were indicative for necrosis. These changes may induce death of hepatocytes either by apoptosis or by necrosis

[31]. The marked dilatation in the blood vessels observed in this work may be due to portal hypertension [32].

This group (IIa Fibrosis) also showed marked increase in collagen fibers in the interlobular septa, portal tracts and in between the hepatocytes cords. Increased collagen level is coinciding with significant increase in  $\alpha$ -SMA expression in activated HSCs which are branched stellate cells situated in between the hepatocytes. So it can be distinguished from other myofibroblasts taking also the same distribution of stained collagen fibers through the affected lobules as in liver injury. HSCs were activated through of TGF- $\beta$ . This cytokine is synthesized by different cell types in liver such as apoptotic hepatocytes and kupffer cells [33].

A few hepatocytes showed immunoreaction for PCNA in the untreated fibrosis group, as hepatocyte replication and regeneration are unique responses of the injured liver [34].

In subgroup IIb (the MSCs-treated group), MSCs were chosen as they have high differentiative abilities with easy accessibility and minimal invasiveness, which makes them more advantageous than other stem cells [26].

Subgroup IIb (the MSCs-treated group) revealed dilated portal vessels and inflammatory cellular infiltration, but these changes were moderate in comparison with those of the untreated fibrosis group. Thick connective tissue septa were seen, but the area% of collagen in this group was significantly lower when compared with that of the untreated fibrosis group. On correlating findings of immunostained sections for  $\alpha$ -SMA, the area% of HSCs was also significantly lower when compared with the untreated fibrosis group. Many hepatocytes had a normal appearance with vesicular nuclei, and some binucleated hepatocytes were also detected. These findings add more evidence to the therapeutic potential of human umbilical MSCs and bone marrow MSCs in the treatment of rat liver fibrosis reported in other previous studies [23,30]. In addition, MSCs may suppress HSC activity and secrete MMPs, thereby eliminating ECM deposition [35].

Many hepatocytes in the MSCs-treated group exhibited nuclear immunoreactivity for PCNA. This increase was significant in comparison with the control group. As reported in other studies, PCNA-positive cells could be proliferating hepatocytes indicating the regeneration of the liver after its injury. PCNA expression increased after human amniotic MSCs transplantation compared with the little PCNA immunostaining in normal livers [36].

In subgroup IIc (the HGF–CNP-treated group), HGF was incorporated in CNP nanoparticles for the delivery of HGF as drug carriers for long-acting medication. That was because HGF has a very short half-life. It is very difficult to sustain a constant high level of exogenous HGF in the circulation [23].

Subgroup IIc (the HGF–CNP treated group) revealed dilated portal vessels and disorganization of the lobular architecture but to a less extent compared with the untreated fibrosis group. There were many normal hepatocytes with vesicular nuclei. A few vacuolated

hepatocytes could be seen. Some hepatocytes with rarified cytoplasm were detected. A few cells with deep acidophilic cytoplasm and small, dark pyknotic nuclei were also noticed. Mild cellular infiltration was detected in between the hepatocytes. These findings denoted improvement in the fibrosis with residual changes. There was thickening of interlobular fibrous septa with increased area% of collagen compared with control but less than that of the untreated fibrosis group, and hence there was a direct relationship between the area% of collagen and  $\alpha$ -SMA immunostaining for HSCs, as HGF has therapeutic potential as an antiapoptotic, anti-inflammatory, and antifibrotic agent, in addition to inhibiting collagen synthesis in HSCs [37]. In this study, many hepatocytes expressed nuclear immunoreactivity for PCNA with significant increase compared with the control group. This can be explained as HGF could promote liver regeneration by enhancing mitosis and inhibiting apoptosis of hepatocytes [38].

Subgroup IId (the MSCs+HGF-CNP-treated group) more or less regained the normal hepatic architecture: cords of vesicular nucleated hepatocytes radiating from the central vein and absence of dilated vessels in the portal tract. A few hepatocytes with dark acidophilic cytoplasm and dark nuclei (feature of apoptotic cells) were detected. Many binucleated hepatocytes could be seen. However, remnants of thin connective tissue septa were found. A minimal amount of collagen fibers were detected around the central vein and in the portal tract, and the area% of collagen was increased compared with the control group and significantly decreased compared with the untreated fibrosis group and the MSCs-treated and HGF-CNP-treated groups. These findings denoted the synergistic effect of mixed MSCs and HGF-CNP in treating liver fibrosis. These results were directly related to the area% of  $\alpha$ -SMA immunoreactivity of HSCs. In addition, many hepatocytes showed PCNA nuclear immunoreactivity with significant increase compared with the control, the untreated fibrosis, the MSCs-treated, and the HGF-CNP-treated groups. These findings were in agreement with those of Jin *et al.* [39].

In the CNP-treated group, many hepatocytes were vacuolated with fragmented nuclei (karyorrhexis). Some cells were apoptotic with deep acidophilic cytoplasm and small, dark pyknotic nuclei. There was marked thickening of the interlobular septa and disorganization of the lobular architecture, with marked increase in the amount of collagen fibers in the interlobular septa, portal tracts, and in between the distorted hepatocyte cords; this increase was significant in comparison with the control, MSCs-treated, HGF-CNP-treated, and MSCs+HGF-CNP-treated groups. There was a statistically significant decrease in the amount of collagen in comparison with the untreated fibrosis group. The area% of  $\alpha$ -SMA immunostaining for HSCs had a direct relationship with the area% of collagen. A few hepatocytes showed immunoreaction for PCNA, which was higher than that of the control group and the untreated fibrosis group. This mild improvement compared with the untreated fibrosis

group may be due to the carrying effect of endogenous HGF [39].

## Acknowledgements

### Conflicts of interest

There are no conflicts of interest.

## References

- Battaller R, Brenner DA, Battaller R, Brenner DA. Liver fibrosis. *J Clin Invest* 2005; 115:209–218.
- Friedman SL. Mechanisms of hepatic fibrogenesis. *Gastroenterology* 2008; 134:1655–1669.
- Sato Y, Araki H, Kato J, Nakamura K, Kawano Y, Kobune M, *et al.* Human mesenchymal stem cells xenografted directly to rat liver are differentiated into human hepatocytes without fusion. *Blood* 2005; 106:756–763.
- Pittenger MF, Mackay AM, Beck SC, Jaiswal RK, Douglas R, Mosca JD, *et al.* Multilineage potential of adult human mesenchymal stem cells. *Science* 1999; 284:143–147.
- Krause DS, Theise ND, Collector MI, Henegariu O, Hwang S, Gardner R, *et al.* Multi-organ, multi-lineage engraftment by a single bone marrow-derived stem cell. *Cell* 2001; 105:369–377.
- Anjos-Afonso F, Siapati EK, Bonnet D. *In vivo* contribution of murine mesenchymal stem cells into multiple cell-types under minimal damage conditions. *J Cell Sci* 2004; 117:5655–5664.
- Kanazawa Y, Verma IM. Little evidence of bone marrow-derived hepatocytes in the replacement of injured liver. *Proc Natl Acad Sci USA* 2003; 100 (Suppl 1):11850–11853.
- Vassilopoulos G, Wang P-R, Russell DW. Transplanted bone marrow regenerates liver by cell fusion. *Nature* 2003; 422:901–904.
- Yeh ETH, Zhang S, Wu HD, Körbling M, Willerson JT, Estrov Z. Transdifferentiation of human peripheral blood CD34<sup>+</sup>-enriched cell population into cardiomyocytes, endothelial cells and smooth muscle cells *in vivo*. *Circulation* 2003; 108:2070–2073.
- Mangi AA, Noiseux N, Kong D, He H, Rezvani M, Ingwall JS, Dzau VJ. Mesenchymal stem cells modified with Akt prevent remodeling and restore performance of infarcted hearts. *Nat Med* 2003; 9:1195–1201.
- Ueki T, Kaneda Y, Tsutsui H, Nakanishi K, Sawa Y, Morishita R, *et al.* Hepatocyte growth factor gene therapy of liver cirrhosis in rats. *Nat Med* 1999; 5:226–230.
- Shiota G, Kunisada T, Oyama K, Udagawa A, Nomi T, Tanaka K, *et al.* *In vivo* transfer of hepatocyte growth factor gene accelerates proliferation of hepatic oval cells in a 2-acetylaminofluorene/partial hepatectomy model in rats. *FEBS Lett* 2000; 470:325–330.
- Kawaida K, Matsumoto K, Shimazu H, Nakamura T. Hepatocyte growth factor prevents acute renal failure and accelerates renal regeneration in mice. *Proc Natl Acad Sci U S A* 1994; 91:4357–4361.
- Ishii T, Sato M, Sudo K, Suzuki M, Nakai H, Hishida T, *et al.* Hepatocyte growth factor stimulates liver regeneration and elevates blood protein level in normal and partially hepatectomized rats. *J Biochem* 1995; 117:1105–1112.
- Roy K, Mao HQ, Huang SK, Leong KW. Oral gene delivery with chitosan-DNA nanoparticles generates immunologic protection in a murine model of peanut allergy. *Nat Med* 1999; 5:387–391.
- Amidi M, Romeijn SG, Borchard G, Junginger HE, Hennink WE, Jiskoot W. Preparation and characterization of protein-loaded *N*-trimethyl chitosan nanoparticles as nasal delivery system. *J Control Release* 2006; 111:107–116.
- Gluck JP, DiPasquale T, Orlans FB. Applied ethics in animal research: Philosophy, regulation and laboratory applications. West Lafayette, IN: Purdue University Press; 2002.
- Alhadlaq A, Mao JJ. Mesenchymal stem cells: isolation and therapeutics. *Stem Cells Dev* 2004; 13:436–448.
- Pan Y, Li YJ, Zhao HY, Zheng JM, Xu H, Wei G, *et al.* Bioadhesive polysaccharide in protein delivery system: chitosan nanoparticles improve the intestinal absorption of insulin *in vivo*. *Int J Pharm* 2002; 249:139–147.
- Kiernan JA. Histological and histochemical methods: theory and practice. 3rd ed. London: Arnold Publisher; 2001.
- Bancroft JD, Cook HC. Immunocytochemistry. In: Bancroft JD, Cook HC, Turner DR, editors. Manual of histological techniques and their diagnostic applications. 2nd ed. New York: Churchill Livingstone; 1994. pp. 263–325.
- Armitage P, Berry G. Statistical methods. In: Armitage P, Berry G (Geoffrey), editors. Medical research. 3rd ed. London: Blackwell Scientific Publications; 1994. pp. 12–48.
- Pulavendran S, Rose C, Mandal AB. Hepatocyte growth factor incorporated chitosan nanoparticles augment the differentiation of stem cell into hepatocytes for the recovery of liver cirrhosis in mice. *J Nanobiotechnology* 2011; 9: 15.
- Waters NJ, Waterfield CJ, Farrant RD, Holmes E, Nicholson JK. Metabonomic deconvolution of embedded toxicity: application to thioacetamide hepatotoxicity and nephrotoxicity. *Chem Res Toxicol* 2005; 18:639–654.
- Alshawsh MA, Abdulla MA, Ismail S, Amin ZA. Hepatoprotective effects of Orthosiphon stamineus extract on thioacetamide-induced liver cirrhosis in rats. *Evid Based Complement Altern Med* 2011; 2011: 103039.

- 26 Zhao W, Li JJ, Cao DY, Li X, Zhang LY, He Y, *et al.* Intravenous injection of mesenchymal stem cells is effective in treating liver fibrosis. *World J Gastroenterol* 2012; 18:1048–1058.
- 27 Roderfeld M, Rath T, Voswinckel R, Dierkes C, Dietrich H, Zahner D, *et al.* Bone marrow transplantation demonstrates medullar origin of CD34<sup>+</sup> fibrocytes and ameliorates hepatic fibrosis in Abcb4<sup>-/-</sup> mice. *Hepatology* 2010; 51:267–276.
- 28 Muhanna N, Tair LA, Doron S, Amer J, Azzeh M, Mahamid M, Friedman S, Safadi R. Amelioration of hepatic fibrosis by NK cell activation. *Gut* 2011; 60:90–98.
- 29 Maga G, Hübscher U. Proliferating cell nuclear antigen (PCNA): a dancer with many partners. *J Cell Sci* 2003; 116:3051–3060.
- 30 Tsai PC, Fu TW, Chen YMA, Ko TL, Chen TH, Shih YH, *et al.* The therapeutic potential of human umbilical mesenchymal stem cells from Wharton's jelly in the treatment of rat liver fibrosis. *Liver Transpl* 2009; 15:484–495.
- 31 Gu K, Zhao JD, Ren ZG, Ma NY, Lai ST, Wang J, *et al.* A natural process of cirrhosis resolution and deceleration of liver regeneration after thioacetamide withdrawal in a rat model. *Mol Biol Rep* 2011; 38:1687–1696.
- 32 Hu LS, George J, Wang JH. Current concepts on the role of nitric oxide in portal hypertension. *World J Gastroenterol* 2013; 19:1707–1717.
- 33 Sobrevals L, Rodríguez C, Romero Trevejo JL, Gondi G, Monreal I, Páneda A, *et al.* Insulin-like growth factor i gene transfer to cirrhotic liver induces fibrolysis and reduces fibrogenesis leading to cirrhosis reversion in rats. *Hepatology* 2010; 51:912–921.
- 34 Wiemann SU, Satyanarayana A, Tsahuridu M, Tillmann HL, Zender L, Klempnauer J, *et al.* Hepatocyte telomere shortening and senescence are general markers of human liver cirrhosis. *FASEB J* 2002; 16:935–942.
- 35 Yannaki E, Athanasiou E, Xagorari A, Constantinou V, Batsis I, Kaloyannidis P, *et al.* G-CSF-primed hematopoietic stem cells or G-CSF per se accelerate recovery and improve survival after liver injury, predominantly by promoting endogenous repair programs. *Exp Hematol* 2005; 33:108–119.
- 36 Zhang D, Jiang M, Miao D. Transplanted human amniotic membrane-derived mesenchymal stem cells ameliorate carbon tetrachloride-induced liver cirrhosis in mouse. *PLoS ONE* 2011; 6:e16789.
- 37 Ogawa T, Iizuka M, Sekiya Y, Yoshizato K, Ikeda K, Kawada N. Suppression of type I collagen production by microRNA-29b in cultured human stellate cells. *Biochem Biophys Res Commun* 2010; 391:316–321.
- 38 Chen Y, Shao JZ, Xiang LX, Dong XJ, Zhang GR. Mesenchymal stem cells: a promising candidate in regenerative medicine. *Int J Biochem Cell Biol* 2008; 40:815–820.
- 39 Jin SZ, Meng XW, Sun X, Han MZ, Liu BR, Wang XH, Pei FH. Hepatocyte growth factor promotes liver regeneration induced by transfusion of bone marrow mononuclear cells in a murine acute liver failure model. *J Hepatobiliary Pancreat Sci* 2011; 18:397–405.

## الملخص العربي

### دراسة هستولوجية عن تأثير الخلايا الجذعية و عامل النمو الكبدي على تليف الكبد المستحث في ذكور الجرذان البيضاء

عبير فؤاد عبد المحسن، نجلاء محمد سلامه، محمد صلاح الجندي<sup>1</sup>،  
أسماء محمد السيد علي<sup>1</sup>

قسم الهستولوجيا - كلية الطب - جامعة القاهرة و<sup>1</sup>جامعة الفيوم

**المقدمة:** تليف الكبد مشكلة صحية مصرية ضخمة. وتعتبر الخلايا النجمية الكبدية ذات دور محوري في حدوثه. وتعتبر الخلايا الجذعية و عامل النمو الكبدي مساهمان رئيسيان في علاجه وتعتبر حبيبات الشيتوزان الدقيقة من وسائل حمل عامل النمو الكبدي إلى البيئة المناسبة لعمله وتأثيره.

**الهدف من الدراسة:** لمقارنة تأثير الخلايا الجذعية و عامل النمو الكبدي إما بشكل منفصل أو مختلطة معا ، في تحسين تليف الكبد المستحث بإستخدام ثيوأسيتاميد في الجرذان البيضاء.

**الأدوات و الطرق المستخدمة:** تم استخدام عدد ستون من ذكور الجرذان البيضاء في هذا العمل . و تم تقسيمها إلى مجموعتين رئيسيتين: مجموعة ضابطة من 10 جرذان و مجموعة تليف الكبد التي تم تقسيمها إلى خمسة مجموعات فرعية بكل منها 10 جرذان:

مجموعة التليف دون علاج

مجموعة الخلايا الجذعية

مجموعة عامل النمو الكبدي المحملة على الشيتوزان

مجموعة الخلايا الجذعية و عامل النمو الكبدي المحملة على الشيتوزان

مجموعة الشيتوزان

و قد تم أخذ عينات من كبد الجرذان و تجهيزها للصبغة بلصبغات التالية:

الهيماتوكسلين و الإيوسين

ماسون ثلاثي الألوان

و الصبغة المناعية للألفا أكتين الخاص بالعضلات الملساء و الصبغة المناعية لمولد المضاد النووي الدال على تكاثر الخلايا.

**النتائج:** حقق إعطاء كل من الخلايا الجذعية الوسطية أو عامل نمو الخلايا الكبدية المندمج بجسيمات الشيتوزان الدقيقة على حدة تحسنا جزئيا في علاج التليف الكبدي المستحث بالثيوأسيتاميد في الفئران. و ذلك من ناحية إستعادة الكبد للشكل العام القريب من الطبيعي و تقليل نسبة الكولاجين و كذلك نقص الصبغة المناعية للألفا أكتين الخاص بالعضلات الملساء و زيادة الصبغة المناعية لمولد المضاد النووي الدال على تكاثر الخلايا بينما كان للخلايا الجذعية الوسطية الممزوجة بعامل نمو الخلايا الكبدية المندمج بجسيمات الشيتوزان الدقيقة دورا علاجيا أفضل في علاج التليف الكبدي في الفئران أكثر من باقى المجموعات فيما حقق حقن الشيتوزان وحده نتائج طفيفة.

**الخلاصة:** كان للخلايا الجذعية الوسطية الممزوجة بعامل نمو الخلايا الكبدية المندمج بجسيمات الشيتوزان الدقيقة الدور العلاجي الأفضل في علاج التليف الكبدي في الفئران أكثر من باقى المجموعات. وفي حال إثبات فاعلية هذا الإتجاه العلاجي على الإنسان فسيصبح اختيارا أمثل لمرضى التليف الكبدي و تقليل الحاجة إلى زراعة الكبد.